Trophic positions of mesozooplankton across the North Atlantic: estimates derived from biovolume spectrum theories and stable isotope analyses

Sünnje L. Basedow[1*], Nuwan A. L. de Silva[2], Antonio Bode[3] and Justus van Beusekorn[4]

[1]UiT – The Arctic University of Norway, Faculty of Biosciences, Fisheries and Economics, Post box 6050, 9037 Tromsø, Norway

[2]University of Canterbury, School of Biological Sciences, Private Bag 4800, Christchurch 8140, New Zealand

[3]Instituto Español de Oceanografía, Centro Oceanográfico de A Coruña Apdo. 130, E-15080, A Coruña, Spain

[4]Universität Hamburg, Institut für Hydrobiologie und Fischereiwissenschaft, Große Elbstraße 133, 22767 Hamburg, Germany

* Corresponding author: sunnje.basedow@uit.no

ABSTRACT

The structure of marine pelagic food webs determines the fate of organic carbon and productivity, but it is difficult to measure. We compared two common methods (stable isotope analyses, SIA, and biovolume spectrum theories, BST) of estimating trophic positions (TP) of mesozooplankton. Two sets of stations across the North Atlantic (Iceland Basin, Irminger Basin, Labrador Sea) were clearly separated. In the East we observed a very early spring bloom, with mixed layer depths > 500 m, chlorophyll *a* evenly distributed, and the *Calanus* population dominated by CV/adults. Here, TPs based on both methods were comparable, with a TP of 2 for small zooplankton and 2-3 for larger species. In the West a more advanced stage of the bloom was observed, with mixed layer depths < 100 m, surface maxima of chlorophyll *a*, higher proportions of young stages of *Calanus*, and more abundant microzooplankton. Here, significant differences in TPs were observed, with those based on BST being about 1 and 3 higher than those based on SIA, for small (TP ~ 3) and large (TP ~ 5) species, respectively. We conclude that biovolume spectrum theories capture energy flow through the microbial food web that is undetected by estimations using stable isotopes.

KEYWORDS: trophic level, zooplankton, North Atlantic, NBSS, spring bloom, microzooplankton

INTRODUCTION

Marine pelagic food webs are complex with numerous linkages between many species that span

several orders of magnitude in size. It is within the planktonic food web that the fate of primary production and organic carbon is determined (Steinberg et al., 2008), and the structure of plankton communities is crucial in determining food chain length and productivity of marine food webs (Sommer et al., 2002; Hunt et al., 2015). Apart from a few specialised organisms most planktonic organisms are opportunistic feeders exhibiting a large degree of omnivory, and also mixotrophy is wide-spread (Link, 2002; Castellani et al., 2008; Zubkov and Tarran, 2008; Mitra et al., 2014). These variable trophic links within plankton communities might stabilise marine pelagic food webs (Schoenly et al., 1991; Link, 2002), but add complexity to the analyses of trophic interactions. The diminutive size of many organisms involved further complicates these analyses. Alone in the so-called microbial part of the marine food web organism size spans four orders of magnitude, from picoplankton to large ciliates.

Resource availability is an important factor determining food chain length in limnic environments (Post, 2002; Doi, 2012). In marine ecosystems at higher latitudes resource availability is strongly coupled to the pronounced seasonality and the development of the phytoplankton bloom.
Of all possible trophic links within the pelagic food web, the number of realised links (connectance) varies over short spatial and temporal scales. In productive areas and during bloom periods important mesozooplankton grazers can feed nearly exclusively herbivorously resulting in a low trophic position (Levinsen et al., 2000; Tamelander et al., 2008; Miller et al., 2010). In oligotrophic areas and outside bloom situations, when microzooplankton is more abundant, grazers might feed more omnivorously and maximum food chain length increases (Runge and de Lafontaine, 1996; Sommer et al., 2002; Fileman et al., 2011; Hunt et al., 2015).

Because of the above mentioned challenges, trophic positions (TP) of planktonic organisms can be determined directly for a few, selected species only. For larger species it is possible to examine the gut content of individuals either by microscopy (Grigor et al., 2014) or by genomic analysis (Durbin et al., 2015), however, the poor conservation of gut contents and the lack of enough genomic information on the potential prey are often limiting factors in their application. Moreover, gut contents offer a snapshot of the actual diet of a particular specimen for a particular time and space, thus requiring a large number of analyses to define the diet and TP of each species. Alternatively, trophic positions can be estimated using indirect methods, which consider zooplankton diet integrated over time and space and allow to estimate the TP for a wider range of species in the food web. Two methods that have been used successfully are the TP estimation based on biomass-size distributions of plankton (Zhou, 2006) and based on the enrichment of natural stable nitrogen

isotopes with TP (Post, 2002).

The estimation of TP based on biomass-size distributions is based on the early observation of a regular distribution of plankton biomass with size (Sheldon et al., 1972), which was followed by the realisation that the shape of the so-called biomass spectrum is determined by fluxes through the pelagic system (Platt and Denman, 1978, Silver and Platt, 1978). The regularities in the size structure of planktonic organisms therefore allow for the estimation of several functional properties of pelagic communities (Edvardsen et al., 2002; Trudnowska et al., 2014). Contemporary mathematical-ecological interpretations of biomass spectra (and the equivalent biovolume spectra) are not based on empirical assumptions (Zhou and Huntley, 1997), however, when estimating TP the biovolume spectrum needs to be linearly on a logarithmic scale and zooplankton assimilation efficiency needs to be set (Zhou, 2006). Alternatively, if the biovolume spectrum is not normalised, residuals can be estimated to identify domes associated to different trophic groups but without the information on their trophic position (Thiebaux and Dickie, 1993; Quintana et al., 2002; Quiroga et al., 2014).

The estimation of TP from stable isotopes is based on the regular increase in the relative abundance of the heavy nitrogen isotope $\delta^{15}N$ with each trophic transfer (Post, 2002). Thus by knowing the values of $\delta^{15}N$ in a given consumer and in a reference TP at the base of the food web it is possible to estimate the TP of the consumer. This approach is now of widespread use in both terrestrial and aquatic food webs (Martínez del Rio et al. 2009; Middelburg, 2014), and there are many examples from marine planktonic communities (e.g. Sommer and Sommer, 2004; Bode et al., 2007; Agersted et al., 2014). The main limitations of this approach, however, are the accurate determination of the reference TP at the base of the food web (Vander Zanden and Rasmussen, 2001) and the existence of different isotopic enrichments between TP (Post, 2002; Hussey et al., 2014).

Within marine pelagic communities, a general increase in $\delta^{15}N$ with zooplankton size is observed, but there are large variations within the mesozooplankton group (Fry and Quinones, 1994; Tarling et al., 2012; Espinasse et al., 2014; Hunt et al., 2015). In the oligotrophic Sargasso Sea a more pronounced in crease in $\delta^{15}N$ compared to the productive systems of Georges Bank and Gulf of Maine was observed (Fry and Quniones, 1994). Seasonal variations in slopes of biomass spectra and $\delta^{15}N$ values show an increase in TPs from spring to summer and autumn (Tarling et al., 2012), but depending on the feeding mode of mesozooplankton also a decrease in TP with size has been

observed (Espinasse et al., 2014). Compared to macrozooplankton and nekton, the increase in TP in the mesozooplankton community is higher, as shown for the sub-tropical Pacific (Hunt et al., 2015). These studies indicate that a larger amount of energy is cycled through the microbial part of the food web in less productive regions and seasons, which is reflected in the TPs estimated for mesozooplankton and might be related to resource availability. Trophic positions of mesozooplankton estimated based on biovolume spectrum theories are higher than comparable estimates based on stable isotopes (Basedow et al., 2010), but to our knowledge there are no published evidences of the performance of different indicators of planktonic TP using different methods, and how these vary in changing productivity conditions

Many of the trophic links within marine pelagic food webs are still barely known, one example is the potential ability of chaetognaths to also use DOM as an alternative energy input (Casanova et al., 2012). Because of the importance of trophic links within food webs for marine productivity, and because of the above mentioned difficulties in estimating trophic positions, we need further knowledge on the performance of available methods. Our objective is to compare estimates of TP of plankton based on biovolume spectrum theories with those based on stable nitrogen isotopes in communities across the North Atlantic contrasting in resource availability.

METHODS

Study area

The North Atlantic has been, and might still be, the most sampled and studied ocean (Marra, 1995). Hence, many oceanographic paradigms originate from studies in the North Atlantic, e.g. ocean seasonality and the deep convection, which permits thermohaline circulation (Talley et al., 2011). The irregular topography that steers thermohaline circulation in combination with the wind-driven circulation in the upper layer results in a complex hydrography of the North Atlantic (Talley et al., 2011). In the upper layer, warm, saline waters enter the North Atlantic Ocean from the Southwest with the North Atlantic Current (NAC) and flow eastwards across the Atlantic and then northwards toward Iceland and Scotland (Fig. 1). A branch of the NAC continues into the Norwegian Sea with the Norwegian Atlantic Current, another flows as the Irminger Current around the Irminger Basin and then into the Labrador Sea. The winter mixed layer depth in the region is very deep (> 400 m), and the characteristic water mass formed through deep convection is generally termed Subpolar Mode Water. The warmest and most saline version is formed in the NAC, it is the water mass following the Irminger Current. Along its way it becomes gradually colder, fresher and denser when

it mixes with Mode water formed further North. Labrador Sea Water (LSW) is the coldest, freshest and densest Mode Water in the region. It is formed in the Labrador and Irminger Sea, and spreads out across the northern North Atlantic, below the warmer mode water types, at intermediate depths down to ca. 1100 m. Also North Atlantic Deep Water (NADW), which is found below ca. 1200 m, is formed in the northern North Atlantic. It forms when LSW mixes with dense and high saline overflow waters flowing over the sills between Greenland and Iceland (Denmark Street Overflow Water) and between Iceland and Scotland (Iceland Scotland Overflow Water), and with dense and high saline Mediterranean Sea (Mediterranean Sea Water), (Morozov et al., 2010).

The pronounced seasonality and the deep convection strongly affect biological processes in the North Atlantic. Deep convection brings new nutrients into surface waters where they can be utilised by primary producers and following by secondary producers after seasonal formation of a thermally stratified surface layer (Siegel et al., 2002). Decoupling and coupling of primary and secondary producers during convective mixing and thermal stratification might initiate and terminate phytoplankton blooms and thus determine primary productivity (Behrenfeld, 2010). Primary production in the North Atlantic has been estimated to be about 12.8 Gt C y^{-1}, or ca. 27 % of the global marine primary production (Carr et al., 2006). Hence, the North Atlantic has been known as a productive system in terms of fisheries, too. This system is subject to accelerating natural and human-induced changes. Climate variability directly and indirectly affects circulation patterns, primary production, secondary production and fish stocks in the North Atlantic (Fromentin and Planque, 1996; Ottersen and Stenseth, 2001; Parsons and Lear, 2001; Beaugrand et al., 2002).

Field sampling

Data on mesozooplankton abundance and biovolume were collected in concert with data on the biophysical environment in the subpolar North Atlantic (from 61.50 °N, 11.00 °W to 59.92 °N, 56.97 °W) during a transatlantic cruise with R/V Maria S. Merian (cruise MSM 26) from Cork, Ireland, to St John's, Canada, in spring 2013 (20 March – 16 April), Fig. 1. Cruise MSM 26 was part of the international EURO-BASIN project, which focused on broad-scale investigations of the North Atlantic pelagic ecosystem, including physical, biogeochemical and biological processes in different habitats.

At 7 stations in the Iceland Basin, Reykjanes Ridge, Irminger Basin and Labrador Sea, respectively, data were collected by a laser optical plankton counter (LOPC; Brooke Ocean, Rolls Royce Ltd, Canada) that was mounted on a rosette-frame together with a conductivity-temperature-depth sensor

(CTD; Seabird 19plusV2, Seabird Electronics Inc., USA) and a fluorescence sensor (F, WETLabs EcoFl, Seabird Electronics Inc., USA). The LOPC-CTD-F instruments were deployed vertically (lowered with 0.7-0.8 m s^{-1}, hauled up with ca. 1 m s^{-1}) from 2000 m at maximum, or 20 to 50 m above bottom, to the surface. Two deployments were carried out at each station, with usually three vertical profiles per deployment (Table 1). The instruments provided quantitative data at a rate of 4 Hz (CTD-F) or 2 Hz (LOPC) on hydrography, fluorescence and on mesozooplankton abundance in the size range between ca. 0.2 and 4 mm equivalent spherical diameter (ESD).

Net samples of two size fractions of zooplankton were collected by vertical hauls in the upper 200 m with a Multinet (55 µm mesh size, 0.25 m^2 mouth opening, Hydro-Bios, Kiel, Germany) and a WP2 (150 µm mesh size, 0.26 m^2 mouth opening). Hauling speed of both nets was between 0.2 to 0.3 m s^{-1}. On deck, the volumes of samples from both nets were brought up to 250 mL with filtered seawater. From both samples, a subsample of 50 mL was immediately fixed in a solution of 4% formaldehyde in seawater for later taxonomic analyses. In case of the 55 µm net, the remaining sample was sieved through a 55 µm sieve, the filtrate then filtered through pre-weighed 47 mm GFA filters, dried at 50 °C for 24 hours and stored for analyses of stable isotopes ashore. The remaining sample from the 150 µm net was first size-fractionated through 2.0 – 1.0 – 0.5 and 0.2 mm sieves and then each fraction was filtered, dried and stored as the sample from the 55 µm net.

Nutrient sampling and analysis

At stations 1, 2 and 9 water samples for nutrient analyses were obtained. Water samples from several depths were filtered into sample tubes through in-line filters (0.45 µm) attached to a syringe. They were kept frozen until analysis. Samples were analyzed with a Seal Analytical Continuous Flow system (AA3) using a variant of the methods in Grashoff et al.. (Grashoff et al., 1983).

Analyses of LOPC-CTD-F data

CTD data were screened for erroneous (out of range) values and then averaged to the same frequency as the LOPC data (2 Hz). Following the recommendations of the Intergovernmental Oceanographic Commission, salinities are reported on the TEOS-10 Absolute Salinity scale and heat content is reported as Conservative Temperature Θ (IOC et al., 2010). Salinity anomalies δS_A were taken from the McDougall et al. (2012) database, version 3.0. Potential density σ_θ was calculated with 0 dbar as reference pressure. All seawater properties were calculated using the Gibbs Seawater package (version 3.0.3) in python. The mixed layer depth was defined as the depth where the difference in potential density compared to σ_θ at surface was 0.03 kg m^{-3}.

Fluorescence was converted into chlorophyll *a* based on a regression from water samples collected with Niskin bottles at 5, 15, 30, 45, 60, 75 and 100 m at station 10 in the Labrador Sea. 250 mL of the samples were filtered on GF/F filters from which chlorophyll *a* concentration was analysed fluorometrically in the laboratory. Fluorescence was determined of the remaining water sample by the fluorescence sensor (F). The resulting regression of fluorescence against chlorophyll *a* ($r^2 = 0.6$, n = 7) yielded relatively high values in bottom waters (> 0.2 mg chl m^{-3}), therefore the mean chlorophyll *a* value of the lower 100 m was subtracted from all values. Due to the low number of filtered samples that was used for the conversion, the resulting chlorophyll *a* values are a rough representation of the true values only.

The laser optical plankton counter measures the size and transparency of particles passing through its sampling channel (Herman et al., 2004). Particles were analysed as described in Basedow et al. (Basedow et al., 2014), and references therein. Analytical steps included (i) computing the particles' size as equivalent spherical diameter (ESD) and digital size, (ii) computing the particles' transparency, (iii) checking the quality of the particles, and (iv) regrouping particles into 49 size classes. Zooplankton abundance of several size groups was then estimated based on particle characteristics and the water volume flowing through the sampling channel. In general, quality of the LOPC data was very good with very few incoherent particles (<0.1%). Erroneous data were detected when the LOPC was not acclimated at surface prior to deployment, these data (upper 300 m of some profiles) were removed and are not included in any further analyses. From all instruments only data from the downcasts were used, because turbulent flow at the top of the instrument carousel might result in incorrect data from the upcasts. For comparison with stable isotope samples, only data from the upper mixed layer were used to compute trophic positions.

Analyses of net samples

Zooplankton species were identified and counted from aliquots of the preserved samples under a stereomicroscope (20x magnification). Specimens were identified to species level where possible and at least 500 individuals were counted from the aliquots. Abundances were computed based on filtered volume assuming 100 % filtration efficiency.

Estimating trophic positions

To enable comparison of trophic positions estimated by stable isotope analyses and biovolume spectrum theories, respectively, LOPC data were grouped into size classes corresponding to the size

fractions obtained by net sampling (Table 3). The size of particles passing through the LOPC is estimated as ESD, i.e. it is the diameter the particle would have if it would be a dark sphere. The ESD therefore does not correspond 1:1 to size fractions obtained by net sampling and sieving. We analysed the taxonomic composition of the size fractions obtained by net sampling, and obtained the ESD of the most abundant species/development stages in each size group based on literature values (Basedow et al., 2014), and references therein. The size fractions obtained by the 0.2 mm and 0.5 mm sieve were grouped together, for a more balanced width of the size groups and to facilitate comparison with the LOPC data.

Biovolume spectrum theories

We estimated trophic positions for the different size groups of the zooplankton community in the North Atlantic following three steps (Basedow et al., 2010). First, we computed the normalised biovolume spectrum *b,* defined as

b = (biovolume in size interval Δw) / (size interval Δw) (in m^{-3}) (1)

with w being the bodyvolume of an individual zooplankton in mm^3. For each station one biovolume spectrum was computed based on the combined data from both deployments of the LOPC, but for the upper layer only (station 1, 2 and 7: upper 500 m, all other stations: upper 200 m). Then, we performed a linear regression analysis (least-squares) of each biovolume spectrum to compute the slope of the spectra. For each biovolume spectrum, one line was fitted to the size range from 0.25 - 4 mm encompassing all size groups but excluding data from the larger size range that were only apparent in the Western region. Three different lines were fitted to each of the size ranges of the zooplankton size groups S, M, and L (Table 3). Due to partly low abundances and the narrow range of size group M, a significant fit of a line could only be obtained for this size group for station 1 (Table 5). At station 10, three unexplained outliers were observed, these were excluded from the linear regression analysis. Finally, we computed the trophic position TP_BST of all size groups for which a significant fit was obtained, based on the slope of the biovolume spectrum b and assuming 70% assimilation efficiency η_n (Zhou 2006, Basedow et al. 2010):

$$TP\_BST = - (1 + \eta_n) / (\delta \ln b / \delta \ln w) \quad (2)$$

Stable isotopes

Natural abundances of stable nitrogen isotopes were determined in plankton size fractions dried previously (50°C, 24h), (Bode et al., 2007). Samples were ground and combusted in an elemental analyser coupled to an Isotope Ratio Mass Spectrometer. These analyses provided values for

nitrogen content and stable isotope abundance ($\delta^{15}N$ standard error of three replicates = 0.06 ‰). Trophic positions derived from these values (TP_SIA) were estimated as in Sommer and Sommer (Sommer and Sommer, 2004):

$$TP\_SIA = [(\delta^{15}N_{sample} - \delta^{15}N_{baseline})/3.4] + 1.5 \quad (3)$$

where $\delta^{15}N_{sample}$ is the isotopic signature of a particular plankton sample fraction and $\delta^{15}N_{baseline}$ the isotopic value of the 55 – 200 µm fraction of the plankton community for the same station as $\delta^{15}N_{sample}$. We assumed that the average increase in $\delta^{15}N$ between adjacent trophic positons was 3.4 ‰ (Post, 2002) and that the TP_SIA of $\delta^{15}N_{baseline}$ was 1.5, representing a mixture of phyto- and zooplankton (Sommer and Sommer, 2004). Estimates of the TP_SIA for the whole zooplankton community were computed using the N-weighted average of $\delta^{15}N$ values of the different size-classes (Landrum et al., 2011).

RESULTS

Hydrography

Greatest differences in water column structure and water mass distribution were observed between the stations east of the Reykjanes Ridge and to the west of it. East of the Reykjanes Ridge and on top of the ridge itself the water column was well-mixed down to more than 500 m (Fig. 2; station 1: 677 m, station 2: 563 m, station 7: 517 m). This thick upper layer had Atlantic Water characteristics with warm temperatures and high salinities. The warmest and most saline waters were observed in the East at station 1 (Θ = 8.6 ºC, S_A = 35.42 g kg^{-1}), and gradually cooler water towards station 7 (Station 2: Θ = 7.8 ºC, S_A = 35.31 g kg^{-1}, station 7: Θ = 7.6 ºC, S_A = 35.32 g kg^{-1}). Below, down to ca. 1200 m, the profiles at station 1 and 2 indicate interleaving of watermasses. At station 1 a salinity minimum above the sill depth of the Faroe Bank Channel (ca. 850 m), (Turrell et al., 1999) might indicate that this water originated from the Faroe Shetland Channel. At the very bottom of station 1, below 1200 m, relatively cold, dense water (Θ < 5.5 ºC, σ_θ > 27.7 kg m^{-3}) was observed, with characteristics similar to those of Iceland Scotland Overflow Water (ISOW), (Talley et al., 2011). West of the Reykjanes Ridge in the Irminger Sea mixed layer depth was shallower, 203 m at station 8, and markedly shallower with 85 m at station 9. Vertical salinity profiles indicate that winter mixing had been down to ca. 500 m at stations 8 and 9 (Fig. 2). Below the upper layer at intermediate depths around 1000 m vertically extensive salinity minima were observed both in the Irminger Sea and in the Labrador Sea. These salinity minima at intermediate depths are typical for Labrador Sea Water (LSW), which was coldest and freshest in the central Labrador Sea at station 10

(Θ = ca. 3.5 ºC, S_A = ca. 35.05 g kg^{-1}). The deepest water masses observed in the Irminger Sea, below ca. 1200 m, were North Atlantic Deep Water (NADW) and Nordic Overflow Waters with 3 ºC < Θ < 4 ºC and S_A > 35.10 g kg^{-1}. In the Labrador Sea, the upper mixed layer was shallow (station 10: 31 m, station 12: 47 m) with low salinities (S_A < 35.0 g kg^{-1}) and low temperatures at station 10. At station 12, however, the upper mixed layer was warmer than at station 10 with in situ temperatures up to 5.4 ºC. This shallow upper layer lay on top of a relatively homogeneous layer down to ca. 500 m in the central Labrador Sea (station 10), and to ca. 200 m at station 12. Below the LSW at intermediate depths, also in the Labrador Sea dense NADW was observed, with Absolute Salinities of 35.09 g kg^{-1} (station 10) and 35.08 g kg^{-1} (station 12), respectively.

Chlorophyll *a*

Chlorophyll *a* (chl *a*) concentrations were low throughout the study area, never exceeding 0.5 mg m^{-3}, but there were notable differences between the stations in the East (1,2 and 7) and the West (9, 10 and 12) with higher values in surface waters in the West, Fig. 2. Lowest chl *a* values in the upper layer were observed east of the Reykjanes Ridge (station 1: 0.07 mg m^{-3}, station 2: 0.14 mg m^{-3}), here chl *a* was distributed more or less homogeneously in the upper mixed layer. Because of the great mixed layer depths east of the ridge and on top of the ridge itself, integrated values of chl *a* over the upper 500 m were comparable at stations 1 (16 mg m^{-2}), 2 (17 mg m^{-2}) and 7 (18 mg m^{-2}) to those stations in the Irminger Sea (17 mg m^{-2} at station 8, 10 mg m^{-2} at station 9) and Labrador Sea (10 mg m^{-2} at station 10, 16 m^{-2} at staton 12). In the Irminger Sea, at station 8 a bimodal peak of chl *a* concentration was observed with a surface maximum of ca. 0.2 mg m^{-3}, and a subsurface maximum around 300 m of ca. 0.08 mg m^{-3}. At station 9 chl *a* concentrations peaked in the upper mixed layer with values close to 0.3 mg m^{-3}. Also in the Labrador Sea chl *a* concentrations peaked in the shallow mixed layer, with ca. 0.2 mg m^{-3} at station 10, and ca 0.4 mg m^{-3} at station 12.

Hydrographical conditions in the East and West of the North Atlantic

Based on the clear differences in hydrographical conditions, two groups of stations were defined: Stations in the East (1, 2 and 7) with MLDs > 500 m and a homogeneous distribution of chl *a* in the mixed layer, and stations in the West (9, 10 and 12) with MLDs < 100 m and surface peaks of chl *a*. Station 8 had intermediate conditions with a MLD of 203 m and a bimodal peak of chl a, it was not included in comparisons between the two groups.

Nutrients and δ^{15}N-baseline

Nutrients at the stations sampled (stations 1, 2 and 9; Table 2) were not reduced at surface compared

to greater depths (data not shown) and the observed values were in the range of reported winter values for the areas (Takahashi et al., 1993; Codispoti et al., 2013). From the stations in the Labrador Sea, nutrient data exist only from station 11 about midway between stations 10 and 12 but not sampled by nets, unfortunately. Here, both nitrate and silicate were reduced in the upper mixed layer (12.72 and 6.10 µmol L^{-1}, respectively) compared to further down (14.25 and 6.88 µmol L^{-1} at 200 m).

The isotopic signature of the $\delta^{15}N_{baseline}$ decreased with increasing chlorophyll at the well-mixed Stations in the East, as expected. In contrast, no relationship between the two parameters was observed at the Stations in the West (Table 2).

Zooplankton community

The zooplankton community sampled by the 55 and 150 µm nets in the upper 200 m consisted mostly of cyclopoid and calanoid copepods, Foraminifera, some meroplanktic larvae and a few chaetognaths (Table 4). Most species had low abundances of less than one individual m^{-3}, with the notable exceptions of *Oithona similis*, *Calanus finmarchicus* and *C. helgolandicus*. *O. similis* was abundant throughout the study area with up to 124 ind. m^{-3}. Lowest abundances (22 ind. m^{-3}) of *O. similis* were observed at the relatively shallow station 7 at the Reykjanes Ridge, where also the lowest abundances in general were recorded. *Calanus* spp. clearly dominated among the 13 species of calanoid copepods, *C. finmarchicus* was more abundant at the stations west of the ridge, and in particular in the Labrador Sea. *C. helgolandicus*, on the other hand, was more abundant east of the ridge with lowest abundances in the Labrador Sea. At station 1 no *Calanus* spp. were observed in the WP2 net sample from the upper 200 m, but data from the 6 LOPC profiles consistently showed older *Calanus* spp. to be evenly distributed in the upper 500 m, with abundances around 300-400 individuals m^{-3} (data not displayed in any figure). The highest numbers of copepod nauplii and younger development stages were observed at stations 12, 9, 8 and 1. The carnivore copepod *Paraeuchaeta norvegica* was relatively abundant (4-6 ind. m^{-3}) at station 2 east of the Midatlantic Ridge, station 8 west of the ridge, and at station 12. Chaetognaths were observed at station 2 in the Iceland basin, station 9 in the Irminger Sea and at station 12. Foraminifera were abundant at station 12, where also the highest abundances of ciliates (*Codonella* spp. and *Favella* spp.) were recorded.

Trophic positions of mesozooplankton in contrasting hydrographical conditions

Based on biovolume spectrum theories

Trophic positions estimated for the mesozooplankton community were generally higher at the stations in the West compared to the stations in the East (Table 6). The trophic positions estimated

for the small zooplankton size group (*Oithona similis*, copepod nauplii, CI *Calanus* spp. and Foraminifera; Table 3) was 1 higher in the West (mean trophic position = 3.2) compared to the East (mean = 2.2), this difference was significant (Student's t-test, $t(4) = 3.9$, $p = 0.02$). For size group M, the trophic position was 2.8 at station 1, and could not be computed for the other stations, see Methods. Marked differences in trophic positions between East and West were observed for the large size group (mainly CV and adult *Calanus* spp., Table 3). Trophic position was significantly higher by about 2.5 in the West (mean trophic position = 5.5) compared to the East (mean = 2.9), Student's t-test, $t(4) = 6.1$, $p = 0.004$.

Based on stable isotope analyses

Trophic positions computed using stable isotopes ranged from 1.6 to 3.5 for the small and large size classes, respectively (Table 6). Average TP-SIA considering all size classes varied between 1.4 (station 2) and 2.3 (stations 1, 7 and 8). No significant difference between stations in the East and in the West were found for any size class (Student's t-test), $p = 0.69$, 0.65, and 0.82, respectively, for the small, medium, and large zooplankton size group.

Differences between the two methods

Looking at the two groups of stations separately, at the stations in the East there was no significant difference in the estimates of trophic positions by stable isotopes analyses or biovolume spectrum theories, neither for the small size group (paired Student's t-test, $t(2) = 0.7$, $p = 0.56$), nor for the large size group ($t(2) = 1.4$, $p = 0.30$), Fig. 4. In contrast, at the stations in the West there was a close to significant difference for the small size group and a very significant difference for the large size group. For the small size group mean estimates of trophic position were 1.1 higher based on biovolume spectrum theories compared to stable isotope analyses (paired Student's t-test, $t(2) = 3.5$, $p = 0.07$). For the large zooplankton group mean trophic positions was 3.2 higher when estimated by biovolume spectrum theories compared to stable isotope analyses (paired Student's t-test, $t(2) = 9.9$, $p = 0.01$).

DISCUSSION

Several studies have employed both stable isotope analyses and biomass/biovolume spectra in the analyses of marine food webs (Jennings et al., 2002; Tarling et al., 2012; Hunt et al., 2015), but to our knowledge this study illustrated for the first time the differences in planktonic trophic position (TP) resulting from estimates based on biovolume spectra and those based on stable isotopes. Across the North Atlantic in spring 2013, two sets of stations were clearly separated by differences

in hydrography, zooplankton community and trophic linkages. In the East, the water column was well-mixed down to ca. 500 m, chl *a* was evenly distributed in the mixed layer, and the *Calanus* population was dominated by CV and adults. Here, TPs based on both methods were about the same, with a TP of ca. 2 for the small size group (mostly *Oithona similis* and Calanoid nauplii) and about 2-3 for the large size group (mostly older stages of *Calanus* spp.). In contrast, in the West, the mixed layer depth was shallow, surface maxima of chl *a* were observed, a higher proportion of young stages of *Calanus* occurred, and microzooplankton was more abundant. Here, significant differences in TPs based on the two methods were observed, with TP_BST being about 1 higher than TP_SIA for the small size group, and about 3 higher for the large size group. This suggests that, in the West, the method based on biovolume spectrum theories tracked energy flow through the planktonic food web that was not detected by stable isotope analyses. Below we discuss reasons for the discrepance between the two methods, and why regional patterns in the estimation of TPs were only observed in TP_BST and not in TP_SIA.

The possibility of high trophic positions of zooplankton

The high TPs estimated for mesozooplankton by biovolume spectrum theories in the West are contradictory to the still popular perception of zooplankton occupying a TP between 2 (herbivorous species) and 3 (carnivorous species), e. g. (Gascuel et al., 2011). They are, however, consistent with our knowledge of diverse linkages within marine microbial food webs (Landry, 2002; Calbet, 2008). For example, a TP of 5 for *Calanus* sp. is expected when it feeds carnivorously on ciliates and when energy flow through the food web is based on particulate organic matter that is recycled by bacteria (Fig. 5). Similar pathways would result in a TP of 6 for carnivorous zooplankton. *Calanus* sp. does feed omnivorously outside bloom situations (Ohman and Runge, 1994; Levinsen et al., 2000; Leiknes et al., 2014), but lipid-class analyses indicate a high degree of herbivory (Falk-Petersen et al., 2009). Therefore, it is more likely that in our study *Calanus* sp. occupied an intermediate TP of 3.5 based on both carnivorous and herbivorous feeding. The large size group was dominated by older stages of *Calanus* sp. but included other mesozooplankton species, because we deliberately chose a wide range for this group in order to compare TPs of the complete mesozooplankton community between the two methods. The high TP_BST estimated for the large group in the West are therefore likely due to in part a omnivorous feeding of *Calanus* sp. and in part a contribution of carnivorous species like chaetognaths or *Paraeuchaeta* sp. to this group.

To estimate TPs based on biovolume spectrum theory a constant assimilation efficiency of 70% was assumed, however, zooplankton assimilation efficiency varies depending on a number

of factors including nutrient content in food, availability of organic compounds, food source, species, body weight, temperature and developmental stage (Mauchline, 1998; Mayzaud et al., 1998; Almeda et al., 2011). As discussed in Basedow et al. (Basedow et al., 2010), estimates of TP based on biovolume spectrum theories do not depend strongly on assimilation efficiency, our estimates therefore can be assumed to give reliable TP_BST with an uncertainty of 0.4 TP at most. Therefore, the lack of correspondence between both methods in estimating TPs in the West must be due to other factors.

Trophic steps in the food web and limitations of stable isotope analyses

One major difficulty when applying TP_SIA estimations to marine plankton is the identification of the baseline (Tamelander et al., 2009). Due to the similarity in size of phytoplankton and heterotroph microzooplankton it is not possible to isolate a sample of pure phytoplankton to characterize $\delta^{15}N$ of primary producers (TP = 1). Alternatively, it is also difficult to identify a first consumer as employed in studies of freshwater food webs (Vander Zanden and Rasmussen, 1999), because most marine zooplankton species are in fact omnivores (Calbet, 2001; Bode et al., 2015). To overcome this difficulty it can be assumed that the size-class selected as baseline represents a fixed mixture of phytoplankton and herbivores (Sommer and Sommer, 2004). This assumption implies that the $\delta^{15}N$ signature of the baseline size-class varies inversely with phytoplankton biomass and directly with heterotrophic biomass. In our study the assumption of a 1:1 mixture of phytoplankton and heterotrophs in the 55 – 200 µm size-class (i.e. TP = 1.5) appears to be applicable in the East where an inverse pattern between $\delta^{15}N$-baseline and chl *a* was observed. Here, no significant differences in TP between both methods were found. This implies also that, in fact, little energy was channelled through the microbial part of the food web at the stations in the East. Otherwise, the heterotrophs in the 55-200 µm size range (lower limited indicated by grey arrowhead in Fig. 5) in all likelihood would have occupied a higher TP (Fig. 5).

In contrast, at the stations in the West, TP_BST of the baseline size-class (size group S) was one level higher than TP_SIA. Here, higher abundances of microzooplankton were observed and the relationship between $\delta^{15}N$-baseline and chl *a* was lost. This suggest that in the West the baseline TP_SIA was higher and likely near 2.5, in line with a mixture of pathways based on both recycled material and on primary producers (Fig. 5). Adjusting the baseline would account for the differences between methods observed for the small plankton group, but would still result in a large difference for the large plankton group. Another potential source of error in estimates of TP_SIA is the variability in enrichment factor. Though constant enrichment factors are generally applicable when

working with simplified food webs (Bode et al., 2007; Hunt et al., 2015), meta-analyses indicate exceptions at lower and higher trophic levels (Vander Zanden and Rasmussen, 2001; Hussey et al., 2014). Furthermore, it has been shown experimentally that trophic steps within the microbial part of the food web are not adequately tracked by variations in $\delta^{15}N$, thus implying that the actual TP is higher than estimated by stable isotope analyses (Gutiérrez-Rodríguez et al., 2014). This is confirmed by our field study indicating higher trophic positions of mesozooplankton in an area with shallow mixed layers, during a time when in all likelihood connectance was high within the planktonic food web. While more research is required to refine the definitions of isotopic baselines and trophic enrichment values, independent TP estimations using size spectra can be used to reveal trophic steps that cannot be accounted for using the current assumptions of constant baselines and trophic enrichment factors.

Trophic coupling prior to the bloom and during pre-bloom

At the stations with deep mixed layer depths in the East we observed relatively low chl a concentrations but high winter nutrient concentrations thus pointing to a very early pre-bloom state of the system. However, chl *a* was distributed homogeneously over the entire mixed layer resulting in areal concentrations that were not insignificant. Here, our data indicate purely herbivorous feeding by the zooplankton community within the mixed layer. This is in line with the dilution-recoupling hypothesis that was proposed by Behrenfeld (Behrenfeld, 2010) based on data from the North Atlantic. He challenged Sverdrup's Critical Depth Hypothesis (Sverdrup, 1953) by stating that the initiation of the phytoplankton spring bloom starts with positive net phytoplankton growth already in winter when MLDs are at maximum. A positive net growth would thus result in an increase in phytoplankton concentrations integrated over the mixed layer, but not necessarily in higher phytoplankton concentrations per m^3 (Behrenfeld, 2010), as was observed in our study. Furthermore, the hypothesis also predicts that, when the MLD ceases to deepen, the coupling between predators and prey is strengthened. Our results of the low trophic position of zooplankton indicate that the coupling between phytoplankton prey and zooplankton predators indeed was strong prior to the bloom and in a deep mixed layer.

With some carefulness, the stations in the West might be characterised as pre-bloom stations, although in the Labrador Sea already young development stages of major grazers were observed. At these stations relatively low chl *a* concentration were concentrated in the shallow surface mixed layer. Nutrient data were only available from a station in roughly the same region as station 10 and 12. They may indicate that nutrient concentrations were just about to start getting reduced in the

Labrador Sea, but not at station 9 in the Irminger Sea. In this situation in the West we already observed high TPs of mesozooplankton, contrary to previous studies based on stable isotopes, which observed high TPs mainly during late bloom and in oligotrophic areas (Søreide et al., 2006; Hunt et al., 2015). Feeding experiments also indicate a higher contribution of microzooplankton to mesozooplankton diet during late bloom and post bloom, which would result in higher TPs, however, feeding on microzooplankton is also observed during pre-bloom although at lower rates (Levinsen et al., 2000). The occurrence of relatively high abundances of CI-CIV *Calanus finmarchicus* at our stations in the West indicates that feeding has been going on for a few weeks, as *C. finmarchicus* needs food for successful spawning and development (Diel and Tande, 1991). In turn, this means that particulate organic matter has been available for some time and microbial linkages within the food web are to be expected. Further evidence is provided by the higher numbers of ciliates present at these stations. Although we cannot clearly delineate the state of the bloom based on the limited data, our results strongly suggest that trophic cycling through the microbial part of the food web was important also during an early phase of the spring bloom.

Implications for energy transfer to higher trophic levels

The high number of TP that were observed in this study influence trophic transfer efficiencies and thus productivity of fisheries (Sommer et al., 2002). Our data suggest that during large parts of the year transfer efficiencies to higher trophic levels might be low, because major amounts of energy are lost during the transfer between micro- and meso-zooplankton. This highlights the importance of the short seasonal periods when phytoplankton biomass is transferred directly to larger zooplankton that are utilised by fish predators. These periods of high transfer efficiencies might well happen prior to the classic spring bloom when high phytoplankton biomass is observed, and rather at times prior to the bloom when phytoplankton growth rate is high, coupling with grazers is strong but cycling through the microbial part of the food web is low.

CONCLUSIONS

We compared estimates of trophic positions of plankton based on biovolume spectrum theories with those based on stable nitrogen isotopes in contrasting regions across the North Atlantic. Based on the high differences in TPs estimated for mesozooplankton in areas with shallow mixed layers, and on additional information on resource availability and the zooplankton community, we conclude that biovolume spectrum theories capture energy flow through the microbial food web that is not detected by estimations based on stable isotopes using current assumptions

Acknowledgements

We thank the captain and crew of R/V M. S. Merian for their assistance during the cruise, Angel F. Lamas for preparing samples for stable isotope analysis, Elena Rey for plankton identification, and Vigdis Tverberg and Boris Espinasse for comments on the manuscript.

Funding

This research was funded in part by the EU Framework Programme 7 (EURO-BASIN, contract No. 264933), the University of Hamburg and the Deutsche Forschungsgemeinschaft.

Data archiving

Raw values of the nitrogen content and stable isotope composition of the samples are stored in the PANGAEA database, http://doi.pangaea.de/10.1594/PANGAEA.837299.

The regrouped LOPC data (49 size classes) are also stored in the PANGAEA database,
station 1: http://doi.pangaea.de/10.1594/PANGAEA.836166,
http://doi.pangaea.de/10.1594/PANGAEA.836165,
station 2: http://doi.pangaea.de/10.1594/PANGAEA.836687,
http://doi.pangaea.de/10.1594/PANGAEA.836689,
station 7: http://doi.pangaea.de/10.1594/PANGAEA.836692,
station 8: http://doi.pangaea.de/10.1594/PANGAEA.836694,
http://doi.pangaea.de/10.1594/PANGAEA.836697,
station 9: http://doi.pangaea.de/10.1594/PANGAEA.836699,
http://doi.pangaea.de/10.1594/PANGAEA.836709,
station 10: http://doi.pangaea.de/10.1594/PANGAEA.836719,
http://doi.pangaea.de/10.1594/PANGAEA.836723,
station 12: http://doi.pangaea.de/10.1594/PANGAEA.836727,
http://doi.pangaea.de/10.1594/PANGAEA.836726.

References

Agersted, M. D., Bode, A., and Nielsen, T. G. (2014) Trophic position of coexisting krill species: a stable isotope approach. *Mar. Ecol. Prog. Ser.,* **516**, 136-151.

Almeda, R., Alcaraz, M., Calbet, A., and Saiz, E. (2011) Metabolic rates and carbon budget of early developmental stages of the marine cyclopoid copepod *Oithona davisae*. *Limnol. Oceanogr*., **56**, 403-414.

Basedow, S. L., Tande, K., and Zhou, M. (2010) Biovolume spectrum theories applied: spatial

patterns of trophic levels within a mesozooplankton community at the polar front. *J. Plankton Res.,* **32**, 1105-1119.

Basedow, S. L, Zhou, M., and Tande, K. S. (2014) Secondary production at the Polar Front, Barents Sea, August 2007. *J. Mar. Sys.*, **130**, 147-159.

Beaugrand, G., Reid, P. C., Ibanez, F., Lindley, J. A., and Edwards, M. (2002) Reorganization of North Atlantic marine copepod biodiversity and climate. *Science*, **296**, 1692-1694.

Behrenfeld, M. J. (2010) Abandoning Sverdrup's Critical Depth Hypothesis on phytoplankton blooms. *Ecology*, **91**, 977-989.

Bode, A., Alvarez-Ossorio, M. T., Cunha, M. E., Garrido, S., Peleteiro, J. B., Porteiro, C., Valdés, L., and Varela, M. (2007) Stable nitrogen isotope studies of the pelagic food web on the Atlantic shelf of the Iberian Peninsula. *Prog. Oceanogr.,* **74**, 115-131.

Bode, M., Hagen, W., Shukat, A, Teuber, L., Fonseca-Batista, D., Dehairs, F., and Auel, H. (2015) Feeding strategies of tropical and subtropical calanoid copepods throughout the eastern Atlantic Ocean – Latitudinal and bathymetric aspects. *Prog. Oceanogr*., **138**, 268-282.

Calbet, A. (2001) Mesozooplankton grazing effect on primary production: A global comparative analysis in marine ecosystems. *Limnol. Oceanogr.*, **46**, 1824-1830.

Calbet, A. (2008) The trophic roles of microzooplankton in marine systems. *ICES J. Mar. Sci.*, **65**, 325-331.

Casanova, J., Barthelemy, R., Duvert, M., Faure, E. (2012) Chaetognaths feed primarily on dissolved and fine particulate organic matter, not on prey: implications for marine food webs. *Hypotheses in the Life Sciences*, **2**, 20-29.

Castellani, C., Irigoien, X., Mayor, D. J., Harris, R. P., and Wilson, D. (2008) Feeding of *Calanus finmarchicus* and *Oithona similis* on the microplankton assemblage in the Irminger Sea, North Atlantic. *J. Plankton Res*., **30**, 1095-1116.

Codespoti, L. A., Kelly, V., Thessen, A., Matrai, P., Suttles, S., Hill, V., Steele, M., and Light, B. (2013) Synthesis of primary production in the Arctic Ocean: III. Nitrate and phosphate based estimates of net community production. *Prog. Oceanogr.,* **110**, 126-150.

Diel, S., and Tande, K. (1992) Does the spawning of *Calanus finmarchicus* in high latitudes follow a reproducible pattern? *Marine Biology*, **113**, 21-31.

Doi, H. (2012) Resource productivity and availability impacts for food-chain length. *Ecol. Res.* **27**, 521-527.

Durbin, E. G., Casas, M. C., and Rynearson, T. A. (2012) Copepod feeding and digestion rates using prey DNA and qPCR. *J. Plankton Res.,* **34**, 72-82.

Edvardsen, A., Zhou, M.,Tande, K. S., and Zhu, Y. (2002) Zooplankton population dynamics:

measuring *in situ* growth and mortality rates using an Optical Plankton Counter. *Mar. Ecol. Prog. Ser.,* **227**, 205-219.

Espinasse, B., Harmelin-Vivien, M., Tiano, M., Guiolloux, L., and Carlotti, F. (2014) Patterns of variations in C and N stable isotope ratios in size-fractionated zooplankton in the Gulf of Lion, NW Mediterranean Sea. *J. Plankton Res.*, **36**, 1204-1215.

Falk-Petersen, S., Mayzaud, P., Kattner, G., and Sargent, J. R. (2009) Lipids and life strategy of Arctic *Calanus*. *Marine Biology Research*, **5**, 18-39.

Fileman, E. S., Fitzgeorge-Balfour, T., Tarran, G. A., and Harris, R. P. (2011) Plankton community diversity from bacteria to copepods in bloom and non-bloom conditions. *Estuarine, Coastal Shelf. Sci.,* **93**, 403-414.

Fromentin, J., and Planque, B. (1996) *Calanus* and environment in the eastern North Atlantic. II. Influence of the North Atlantic Oscillation on *C. finmarchicus* and *C. helgolandicus*. *Mar. Ecol. Prog. Ser.,* **134**, 111-118.

Fry, B., and Quiñones, R. B. (1994) Biomass spectra and stable isotope indicators of trophic level in zooplankton of the northwest Atlantic. *Mar. Ecol. Prog. Ser.*, **112**, 201-204.

Gascuel, D., Guénette, S., and Pauly, D. (2011) The trophic-level-based ecosystem modelling approach: theoretical overview and practical uses. *ICES J. Mar. Sci.*, **68**, 1403-1416.

Grasshoff, K., M. Erhardt, and Kremling, K. (1983) Methods of Seawater Analysis. Verlag Chemie, Weinheim.

Grigor, J. J., Marais, A. E., Falk-Petersen, S., and Varpe, Ø. (2014) Polar night ecology of a pelagic predator, the chaetognath *Parasagitta elegans*. *Polar Biol.,* **38**, 87-98.

Gutiérrez-Rodríguez, A., Décima, M., Popp, B. N., and Landry, M. R. (2014) Isotopic invisibility of protozoan trophic steps in marine food webs. *Limnol. Oceanogr.*, **59**, 1590-1598.

Herman, A. W., Beanlands, B., and Phillips, E. F. (2004) The next generation of Optical Plankton Counter: the Laser-OPC. *J. Plankton Res*., **26**, 1135-1145.

Hunt, B. P. V., Allain, V., Menkes, C., Lorrain, A., Graham, B., Rodier, M., Pagano, M., and Carlotti, F. (2015) A coupled stable isotope-size spectrum approach to understanding pelagic food-web dynamics: A case study from the southwest sub-tropical Pacific. *Deep Sea Res., Part II,* **113**, 208-224.

Hussey, N. E., MacNell, M. A., McMeans, B. C., Ollin, J. A., Dudley, S. F. J., Cliff, G., Winter, S. P., Fennessy, S. T., and Fisk, A. T. (2014) Rescaling the trophic structure of marine food webs. *Ecology Letters,* **17**, 239-250.

Jennings, S., Greenstreet, S. P. R., Hill, L., Piet, G. J., Pinnegar, J. K., and Warr, K. J. (2002) Long-term trends in the trophic structure of the North Sea fish community: evidence from stable-isotope

analysis, size-spectra and community metrics. *Marine Biology*, **141**, 1085-1097.
Landrum, J. P., Altabet, M. A., Montoya, J. P. (2011) Basin-scale distribution of stable nitrogen isotopes in the subtropical North Atlantic: Contribution of diazotroph nitrogen to particulate organic matter and mesozooplankton. *Deep Sea Res*., *Part II*, **58**, 615-625.
Landry, M. R. (2002) Integrating classical and microbial food web concepts: evolving views from the open-ocean tropical Pacific. *Hydrobiologia*, **480**, 29-39.
Leiknes, Ø., Striberny, A., Tokle, N. E., Olsen, Y., Vadstein, O., and Sommer, U. (2014) Feeding selectivity of *Calanus finmarchicus* in the Trondheimsfjord. *J. Sea Res.*, **85**, 292-299.
Levinsen, H., Turner, J. T., Nielsen, T. G., and Hansen, B. W. (2000) On the trophic coupling between protists and copepods in arctic marine ecosystems. *Mar. Ecol. Prog. Ser.*, **204**, 65–77.
Link, J. (2002) Does food web theory work for marine ecosystems? *Mar. Ecol. Prog. Ser*., **230**, 1-9.
Marra, J. (1995) Primary production in the North Atlantic: measurements, scaling, and optical determinants. *Philos. Trans. R. Soc., B*, **348**, 153 - 160.
Martínez del Rio, C., Wolf, N., Carleton, S. A., and Gannes, L. Z. (2009) Isotopic ecology ten years after a call for more laboratory experiments. *Biological Reviews,* **84**, 91-111.
Mauchline, J. (1998) The biology of calanoid copepods. Academic Press, San Diego, USA.
Mayzaud, P., Tirelli, V., Bernard, J. M., and Roche-Mayzaud, O. (1998) The influence of food quality on the nutritional acclimation of the copepod *Acartia clausi*. *J. Mar. Sys*., **15**, 483-494.
McDougall, T. J., Jackett, D. R., Millero, F. J., Pawlowicz, R., and Barker, P. M. (2012) A global algorithm for estimating Absolute Salinity. *Ocean Sci.*, **8**, 1123-1134.
Middelburg, J. J. (2014) Stable isotopes dissect aquatic food webs from the top to the bottom. *Biogeosciences*, **11**, 2357-2371.
Miller, T. W., Brodeur, R. D., Rau, G., and Ornori, K. (2010) Prey dominance shapes trophic structure of the northern California Current pelagic food web: evidence from stable isotopes and diet analysis. *Mar. Ecol. Prog. Ser.*, **420**, 15-26.
Mitra, A., Flynn, K. J., Burkholder, J. M., Berge, T., Calbet, A., Raven, A., Granélli, E., Gilbert, P. M. et al. (2014) The role of mixotrophic protists in the biological carbon pump. *Biogeosciences* **11**, 995-1005.
Morozov, E. G., Demidov, A. N., Tarakanov, R. Y., and Zenk, W. (2010) Abyssal Channels in the Atlantic Ocean: Water Structure and Flows. Springer, New York, USA.
Ohman, M. D., and Runge, J. A. (1994) Sustained fecundity when phytoplankton resources are in short supply: Omnivory by *Calanus finmarchicus* in the Gulf of St. Lawrence. *Limnol. Oceanogr.*, **39**, 21-36.
Ottersen, G., and Stenseth, N. C. (2001) Atlantic climate governs oceanographic and ecological

679 variability in the Barents Sea. *Limnol. Oceanogr*., **46**, 1774-1780.
680 Parsons, L. S., and Lear, W. H. (2001) Climate variability and marine ecosystem impacts: a North
681 Atlantic perspective. *Prog. Oceanogr*., **49**, 167-188.
682 Platt, T., and Denman, K. (1978) The structure of pelagic marine ecosystems. *Rapp. P.-V. Reun. -*
683 *Cons. Int. Explor. Mer.,* **173**, 60–65.
684 Post, D. M. (2002) Using stable isotopes to estimate trophic position: models, methods, and
685 assumptions. *Ecology*, **83**, 703– 718.
686 Quintana, X., Comin, F., and Moreno-Amichi, R. (2002) Biomass-size spectra in aquatic
687 communities in shallow fluctuation Mediterranean salt marshes (Emporda Wetlands, NE Spain). *J.*
688 *Plankton Res.*, **24**, 1149-1161.
689 Quiroga, E., Gerdes, D., Montiel, A., Knust, R. and Jacob, U. (2014) Normalized biomass size
690 spectra in high Antarctic macrobenthic communities: linking trophic position and body size. *Mar.*
691 *Ecol. Prog. Ser*., **506**, 99-113.
692 Runge, J. A., and de Lafontaine, Y. (1996) Characterizaton of the pelagic ecosystem in surface
693 waters of the northern Gulf of St. Lawrence in early summer: the larval redfish-*Calanus*-
694 microplankton interaction. *Fisheries Oceanography*, **5**, 21-37.
695 Schoenly, K., Beaver, R. A., and Heumier, T. A. (1991) On the trophic relations of insects: a food-
696 web approach. *Am. Nat.* **137**, 597-638.
697 Sheldon, R. W., Prakash, A., and Sutcliffe, W. H. J (1972) The size distribution of particles in the
698 ocean. *J. Limnol. Oceanogr.*, **17**, 327–340.
699 Siegel, D. A., Doney, S. C., and Yoder, J. A. (2002) The North Atlantic spring phytoplankton bloom
700 and Sverdrup's critical depth hypothesis. *Science*, **296**, 730-733.
701 Silvert, W. and Platt, T. (1978) Energy flux in the pelagic ecosystem: a time dependent equation.
702 *Limnol. Oceanogr.*, **23**, 813– 816.
703 Sommer, U., Stibor, H., Katechakis, A., Sommer, F., and Hansen, T. (2002) Pelagic food web
704 configurations at different levels of nutrient richness and their implications for the ratio fish
705 production: primary production. *Hydrobiologia* **484**, 11-20.
706 Sommer, F., and Sommer, U. (2004) delta N-15 signatures of marine mesozooplankton and seston
707 size fractions in Kiel Fjord, Baltic Sea. *J. Plankton Res.*, **26**, 495-500.
708 Søreide, J., Hop, H., Carroll, M. L., Falk-Petersen, S., Hegseth, E. N. (2006) Seasonal food web
709 structures and sympagic-pelagic coupling in the European Arctic revealed by stable isotopes and a
710 two-source food web model. *Prog. Oceanogr.*, **71**, 59-87.
711 Steinberg, D.K., Copel, J.S., Wilson, S.E., and Kobari, T. (2008) A comparison of mesopelagic
712 mesozooplankton community structure in the subtropical and subarctic North Pacific Ocean.

713 *Deep-Sea Res., Part II,* **55**, 1615-1635.
714 Sverdrup, H. U. (1953) On conditions for the vernal blooming of phytoplankton. *Journal du*
715 *Conseil International pour l'Exploration de la Mer*, **18**, 287-295.
716 Takahashi, T., Olafson, J., Goddard, J. G., Chipman, D. W., and Sutherland, S. C. (1992) Seasonal
717 variations of CO_2 and nutrients in the high-latitude surface oceans: a comparative study. *Global*
718 *Biogeochemical Cycles*, **7**, 843-878.
719 Talley, L. D., Pickard, G. L., Emery, W. J., and Swift, J. H. (2011) Descriptive physical
720 oceanography, an introduction. Academic Press, Elsevier, London, UK. 6th edition.
721 Tamelander, T., Reigstad, M., Hop, H., Carroll, M. L., and Wassmann, P. (2008) Pelagic and
722 sympagic contribution of organic matter to zooplankton and vertical export in the Barents Sea
723 marginal ice zone. *Deep-Sea Res., Part II*, **55**, 2330–2339.
724 Tamelander, T., Kivimäe, C., Bellerby, R. G. J., Renaud, P. E., and Kristiansen, S. (2009) Base-line
725 variations in stable isotope values in an Arctic marine ecosystem: effects of carbon and nitrogen
726 uptake by phytoplankton. *Hydrobiologia*, **630**, 63-73.
727 Tarling, G. A., Stowasser, G., Ward, P., Poulton, A. J., Zhou, M., and Venables, H. J. (2012)
728 Seasonal trophic structure of the Scotia Sea pelagic ecosystem considered through biomass spectra
729 and stable isotope analysis. *Deep-Sea Res., Part II*, **59-60**, 222-236.
730 Thiebaux, M. L., and Dickie, L. M. (1993) Structure of the body-size spectrum of the biomass in
731 aquatic ecosystems – a consequence of allometry in predator-prey interactions. *Can. J. Fish. Aquat.*
732 *Sci*., **50**, 1308-1317.
733 Turrell, W. R., Slesser, G., Adams, R. D., Payne, R., and Gillibrand, P. A. (1999) Decadal variability
734 in the composition of Faroe Shetland Channel bottom water. *Deep-Sea Res., Part I*, **46**, 1-25.
735 Trudnowska, E., Basedow, S. L., and Blachowiak-Samolyk, K. (2014) Mid-summer
736 mesozooplankton biomass, its size distribution, and estimated production within a glacial Arctic
737 fjord (Hornsund, Svalbard). *J. Mar. Sys.,* **137**, 55-66.
738 Vander Zanden, M. J., and Rasmussen, J. B. (2001) Variation in d15N and d13C trophic
739 fractionation: Implications for aquatic food web studies. *Limnol. Oceanogr.,* **46**, 2061-2066.
740 Zhou, M., and Huntley, M. (1997) Population dynamics theory of plankton based on biomass
741 spectra. *Mar. Ecol. Prog. Ser.*, **159**, 61–73.
742 Zhou, M. (2006) What determines the slope of a plankton biomass spectrum? *J. Plankton Res*., **28**,
743 437-448.
744 Zubkov, M. V,. and Tarran, G. A. (2008) High bacterivory by the smallest phytoplankton in the
745 North Atlantic Ocean. *Nature* **455**, 224-226.
746

Table legends

Table 1. Stations sampled during a cruise with R/V M. S. Merian across the North Atlantic in spring 2013. Vertical profiles (three per haul unless stated otherwise) on zooplankton distribution were obtained from 20 to 50 m above bottom (max. 2000 m) to surface with a laser optical plankton counter (LOPC). The mesozooplankton community was collected with a Multinet (MN, 55 µm mesh size) and a WP2 (150 µm mesh size) by vertical net hauls from 200 m to surface. No Multinet sampling was possible at station 2 due to bad weather, therefore the Multinet sampling from station 1, which was located in the same water mass, was used as the baseline for the stable isotope analyses from station 2. $^{+}$Down to 300 m only. ^{1}Only one profile, ^{2}only two profiles obtained.

Table 2. Nutrient concentrations (µmol L^{-1}) at surface (10 m) and chlorophyll *a* concentrations (mg m^{-2}) integrated over the upper 200 m at 7 stations in the North Atlantic in March/April 2013. For locations of stations see Fig. 1 and Table 1. nd = no data. Δ^{15}N-baseline

Table 3. Classification of size groups applied to data collected in the upper 200 m at 7 stations in the North Atlantic in March/April 2013, by laser optical plankton counter data (given in mm equivalent spherical diameter), and by zooplankton nets for stable isotope analyses (mesh size). Based on species information from the net samples (Table 4) and on literature values of the species' ESD.

Table 4. Zooplankton species composition in the upper 200 m at 7 stations in the North Atlantic in March/April 2013. For locations of stations see Fig. 1 and Table 1. Abundances are in individuals m^{-3}. - = no individual observed, nd = no data available.

Table 5. Parameters of the linear regression lines fitted to biovolume spectra that were obtained from data collected by a laser optical plankton counter in the upper layer at 7 stations in the North Atlantic in March/April 2013. For locations of stations see Fig. 1 and Table 1

Table 6. Trophic positions of the mesozooplankton community in the upper layer at 7 stations across the North Atlantic in spring 2013. Estimates for different size groups (S, M, L, All) were obtained from stable isotope analysis (SIA) and biovolume spectrum theories (BST), respectively. No trophic positions for BST were computed if the fit of the regression line to the biovolume spectrum was not significant (ns) at a level of $p < 0.05$, see Table 5.

780 **Figure legends**

781 Figure 1. Study area showing the placement of stations (yellow triangles) and the main currents
782 (after Talley et al. 2011). Red: North Atlantic current flowing northeastwards across the Atlantic
783 with branches continuing into the Norwegian Sea (Norwegian Atlantic Current) and around the
784 Irminger Sea (Irminger Current) and Labrador Sea. Blue: Overflow water coming from the northern
785 basins and forming the Deep Water Bottom Current. White: Labrador Sea Water that spreads out at
786 intermediate depths in the North Atlantic. Orange: East Greenland Current, West Greenland Current
787 and Labrador Current. Stations were placed in the Iceland Basin (1 and 2), on top of the Reykjanes
788 Ridge (7), in the Irminger Sea (8 and 9), and in the Labrador Sea (10 and 12).
789

790 Figure 2. Vertical profiles of Conservative Temperature (ºC, red), Absolute Salinity (g kg^{-1}, blue),
791 chlorophyll *a* (mg m^{-3}, green) and potential density (kg m^{-3}, black) at 7 stations in the North Atlantic
792 in March/April 2013. Y-axis: Depth (m). Note the difference in axis scales. For positions of stations
793 see Fig. 1 and Table 1.
794

795 Figure 3. Biovolume spectra of the mesozooplankton community in the upper layer (upper 500 m:
796 stations 1, 2 and 7, upper 200 m: all other stations) in spring 2013 in the North Atlantic. Spectra
797 were computed based on data collected along vertical profiles by a laser optical plankton counter,
798 for details see Methods. For locations of stations see Fig. 1 and Table 1.
799

800 Figure 4. Differences in trophic positions estimated by biovolume spectrum theories and stable
801 isotopes analyses, respectively. Differences are shown for small (S) and large (L) mesozooplankton
802 size groups in the upper layer at different stations in the North Atlantic in spring 2013. Stations in
803 the West with a mixed layer depth (MLD) < 100 m and a surface maximum of chlorophyll a (chl a)
804 are separated by dashed lines from stations in the East, where MLD was > 500 m and where chl a
805 was distributed homogeneously within the mixed layer.
806

807 Fig. 5 Basic food web with general key players in the marine pelagic and some of the observed
808 species at our stations in the North Atlantic. Several trophic pathways (black) and recycling paths
809 (grey) are shown, but by no means all. Mean sizes for the different groups are indicated, but ranges
810 are not given, these can be large for e.g. diatoms and ciliates. Small numbers indicate trophic
811 positions. As an example two common pathways resulting in different trophic positions for *Calanus*
812 are highlighted: a carnivorous pathway (red) from particulate organic matter (POM) over
813 heterotrophic bacteria (h-bact), heterotrophic nanoflagellates (h-nan) and ciliates, resulting in a

trophic position of 5, and a herbivorous pathway (green) from diatoms directly to *Calanus*, resulting in a trophic position of 2. Many other pathways are possible. The grey arrowhead indicates the baseline of TP = 1.5 for stable isotope analyses.

Table 1

Region	Station	Gear	Lat (°N)	Lon (°W)	Bottom depth (m)	Date	UTC
Iceland	1_126	LOPC	61.50	11.00	1333	25 Mar	01:05
Basin		WP2	61.50	11.00	1332	25 Mar	04:35
East		LOPC	61.44	10.87	1216	25 Mar	16:41
		MN	61.45	10.86	1221	25 Mar	20:12
Iceland	2_127	WP2	62.82	21.36	1147	28 Mar	05:19
Basin		LOPC	62.82	21.36	1149	28 Mar	06:49
West		LOPC	62.86	21.44	1134	28 Mar	23:20
Reykjanes	7_132	LOPC	61.64	27.04	749	01 Apr	02:07
Ridge		MN	61.64	27.04	755	01 Apr	07:57
		WP2	61.64	27.04	765	01 Apr	08:30
Irminger	8_133	LOPC	62.40	29.53	1943	02 Apr	09:37
Basin		LOPC	62.40	29.53	1949	02 Apr	22:10
North		MN	62.40	29.53	1946	03 Apr	02:32
		WP2	62.40	29.53	1949	03 Apr	02:51
Irminger	9_134	WP2	60.54	34.31	3010	04 Apr	13:17
Basin		MN	60.54	34.31	3002	04 Apr	14:05
South		LOPC	60.54	34.31	3002	05 Apr	00:25
		LOPC	60.54	34.31	2954	05 Apr	11:25[1]
Labrador	10_135	WP2	59.89	55.85	3161	08 Apr	14:24
Basin		MN	59.89	55.85	3158	08 Apr	15:03
Centre		LOPC	59.93	55.98	3151	09 Apr	00:45[2]
		LOPC	59.87	55.74	3171	09 Apr	17:00
Labrador	12_137	MN	53.36	46.77	3810	13 Apr	08:20
Basin		WP2	53.36	46.77	3808	13 Apr	08:51
South		LOPC	53.36	46.77	3811	13 Apr	09:22[+]
		LOPC	53.36	46.77	3811	13 Apr	09:42
		LOPC	53.36	46.77	3807	14 Apr	02:50[2]

Table 2

Station	NO_3^-	NO_2^-	SiO_4^{4-}	PO_4^{3-}	Chl *a*	δ^{15}N-baseline
1	12.63	0.02	4.45	0.39	13.2	3.51
2	11.15	0.03	4.60	0.73	28.3	3.24
7	nd	nd	nd	nd	38.4	2.89
8	nd	nd	nd	nd	42.1	1.53
9	14.09	0.02	6.33	0.97	57.6	2.77
10	nd	nd	nd	nd	34.5	3.71
12	nd	nd	nd	nd	0.2	2.08

Table 3

Size group	LOPC data (mm ESD)	Stable isotope analyses (mm mesh size)	Main species/groups based on net samples
S	0.25 – 0.6	0.2 – 1.0	*Oithona similis*, Copepoda nauplii, *Calanus* spp. CI, Foraminifera
M	0.6 – 1.0	1.0 – 2.0	*Calanus* spp. CII-CII, Calanoida
L	1.0 – 4.0	> 2.0	*Calanus* spp. CIV to adults, *Paraeuchaeta norvegica,*

Table 4

Species/group	**Station 1**	**2**	**7**	**8**	**9**	**10**	**12**
150 µm net							
Copepoda nauplii	5	2	0.3	3	4	3	5
Copepoda CI-CIV	12	-	0.4	16	11	9	14
Calanus finmarchicus	-	3	-	4	9	17	19
C. helgolandicus	-	14	0.4	7	7	4	3
C. hyperboreus	-	-	-	-	-	-	0.2
sum Calanus *spp.*	-	*16*	*0.4*	*11*	*16*	*21*	*22*
Mesocalanus tenuicornis	-	-	-	1	1	-	-
Rhincalanus nasutus	0.2	-	-	-	-	-	-
Clausocalanus spp.	0.2	2	-	-	-	-	-
Ctenocalanus vanus	0.5	-	-	-	-	-	-
Paraeuchaeta norvegica	-	6	-	4	1	-	4
P. hebes	0.3	-	-	-	-	-	-
Metridia lucens	-	1	0.2	-	-	-	-
Pleuromamma robusta	-	-	-	0.3	-	-	-
Centropages chierchiae	-	-	-	-	-	0.4	-
Candacia armata	-	-	-	-	0.2	-	0.7
sum other Calanoida	*1*	*9*	*0.2*	*5*	*2*	*0.4*	*5*
Oithona similis	69	124	22	71	75	36	72
O. nana	-	-	-	2	-	0.2	0.7
O. plumifera	3	2	-	-	3	0.2	-
Oncaea media	-	-	-	0.7	-	-	-
Oncaea spp.	0.9	-	-	-	-	-	2
Euterpina acutifrons	-	-	0.2	-	-	-	-
Microsetella rosea	1	1	-	0.4	0.4	0.3	-
Cladocera	0.2	-	-	-	-	0.3	-
Ostracoda	-	0.1	-	-	0.3	3	3
Cirripedia nauplii	-	-	-	-	-	0.2	-
Decapoda larvae	2	-	-	1	-	0.2	-
Euphausiaceae larvae	-	-	-	-	-	-	4
Amphipoda	-	-	-	0.2	-	-	0.2
Foraminifera	5	-	-	-	-	0.4	4
Siphonophora	-	-	-	0.2	-	-	0.9
Echionodermata larvae	0.2	3	0.2	-	-	-	-
Chaetognatha	-	2	-	-	0.3	-	2
Salpidae	-	0.3	-	-	-	-	-
Pteropoda	-	-	-	-	-	-	0.2
Gastropoda larvae	-	-	0.2	-	-	-	0.9
Polychaeta larvae	-	-	-	0.6	-	-	-
55 µm net							
Copepoda nauplii	52	nd	18	228	248	47	360
Calanoida	0.4	nd	-	13	73	0.6	118
Cyclopoida	5	nd	0.8	19	66	1	158
Harpactoida	1	nd	1	20	21	0.4	5
Foraminifera	0.1	nd	1	-	4	3	123
Tintinnida	-	nd	0.5	4	6	0.6	21
Gastropoda larvae	0.3	nd	-	-	-	-	22
Polychaeta larvae	0.1	nd	-	-	-	-	-

Table 5

Station	Size group	Intercept	Slope	r^2	p-value
1	S	0.03	-1.20	0.97	<0.001
	M	0.23	-0.86	0.84	0.028
	L	0.33	-0.78	0.95	<0.001
	All	0.35	-0.95	0.97	<0.001
2	S	0.32	-1.03	0.95	<0.001
	M	1.11	-0.17	0.17	0.492
	L	1.27	-1.14	0.89	<0.001
	All	0.90	-0.70	0.88	<0.001
7	S	0.12	-1.10	0.95	<0.001
	M	0.75	-0.21	0.19	0.466
	L	0.86	-0.72	0.78	0.001
	All	0.75	-0.66	0.89	<0.001
8	S	0.83	-0.93	0.94	<0.001
	M	1.55	-0.08	0.07	0.674
	L	1.48	-0.92	0.57	0.003
	All	1.27	-0.67	0.81	<0.001
9	S	1.12	-0.82	0.91	<0.001
	M	2.17	+0.12	0.19	0.459
	L	1.83	-0.44	0.84	<0.001
	All	1.80	-0.41	0.91	<0.001
10	S	1.34	-0.66	0.90	<0.001
	M	1.24	-0.88	0.98	0.091
	L	1.86	-0.42	0.62	0.002
	All	1.78	-0.36	0.83	<0.001
12	S	1.90	-0.83	0.94	<0.001
	M	2.51	-0.18	0.41	0.245
	L	2.34	-0.47	0.96	<0.001
	All	2.36	-0.52	0.97	<0.001

Table 6

Station	Size group	SIA	BST
1	S	2.3	2.0
	M	2.2	2.8
	L	2.7	3.1
	All	2.3	2.5
2	S	1.6	2.3
	M	1.5	ns
	L	1.2	2.1
	All	1.4	3.4
7	S	2.0	2.1
	M	2.8	ns
	L	3.5	3.4
	All	2.3	3.7
8	S	2.0	2.6
	M	2.2	ns
	L	2.7	2.7
	All	2.3	3.6
9	S	1.9	3.0
	M	1.7	ns
	L	2.4	5.5
	All	2.0	6.0
10	S	2.0	3.7
	M	2.2	ns
	L	2.0	5.8
	All	2.1	6.7
12	S	2.3	2.9
	M	2.0	ns
	L	2.5	5.2
	All	2.2	4.7

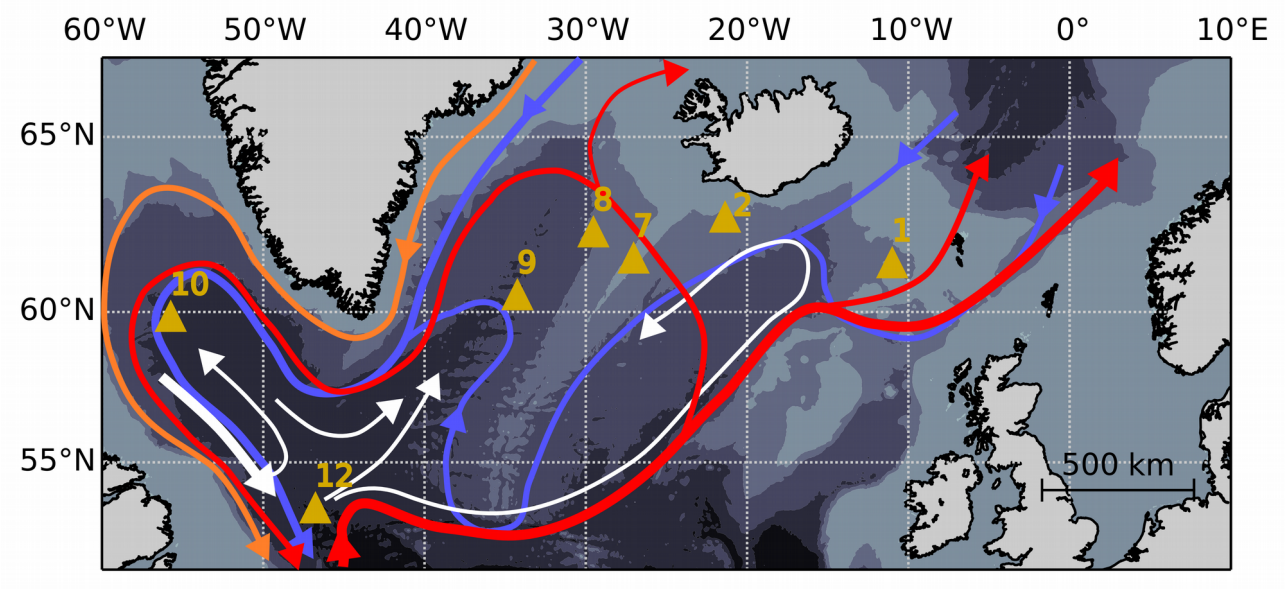

996 Figure 1

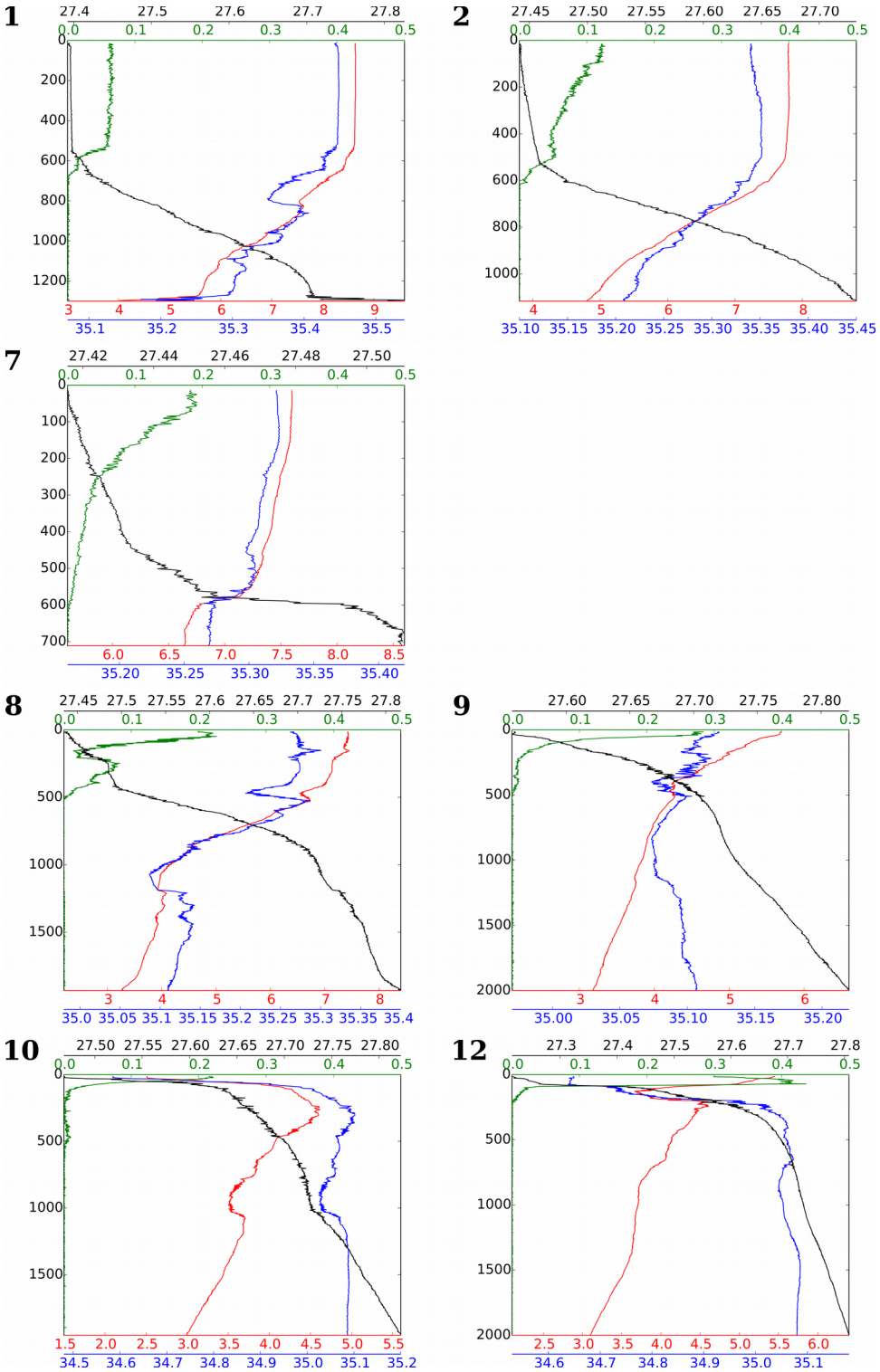
1
27.4 27.5 27.6 27.7 27.8
0.0 0.1 0.2 0.3 0.4 0.5
0 200 400 600 800 1000 1200
3 4 5 6 7 8 9
35.1 35.2 35.3 35.4 35.5
2
27.45 27.50 27.55 27.60 27.65 27.70
0.0 0.1 0.2 0.3 0.4 0.5
0 200 400 600 800 1000
4 5 6 7 8
35.10 35.15 35.20 35.25 35.30 35.35 35.40 35.45
7
27.42 27.44 27.46 27.48 27.50
0.0 0.1 0.2 0.3 0.4 0.5
0 100 200 300 400 500 600 700
6.0 6.5 7.0 7.5 8.0 8.5
35.20 35.25 35.30 35.35 35.40
8
27.45 27.5 27.55 27.6 27.65 27.7 27.75 27.8
0.0 0.1 0.2 0.3 0.4 0.5
0 500 1000 1500
3 4 5 6 7 8
35.0 35.05 35.1 35.15 35.2 35.25 35.3 35.35 35.4
9
27.60 27.65 27.70 27.75 27.80
0.0 0.1 0.2 0.3 0.4 0.5
0 500 1000 1500 2000
3 4 5 6
35.00 35.05 35.10 35.15 35.20
10
27.50 27.55 27.60 27.65 27.70 27.75 27.80
0.0 0.1 0.2 0.3 0.4 0.5
0 500 1000 1500
1.5 2.0 2.5 3.0 3.5 4.0 4.5 5.0 5.5
34.5 34.6 34.7 34.8 34.9 35.0 35.1 35.2
12
27.3 27.4 27.5 27.6 27.7 27.8
0.0 0.1 0.2 0.3 0.4 0.5
0 500 1000 1500 2000
2.5 3.0 3.5 4.0 4.5 5.0 5.5 6.0
34.6 34.7 34.8 34.9 35.0 35.1

998 Figure 2

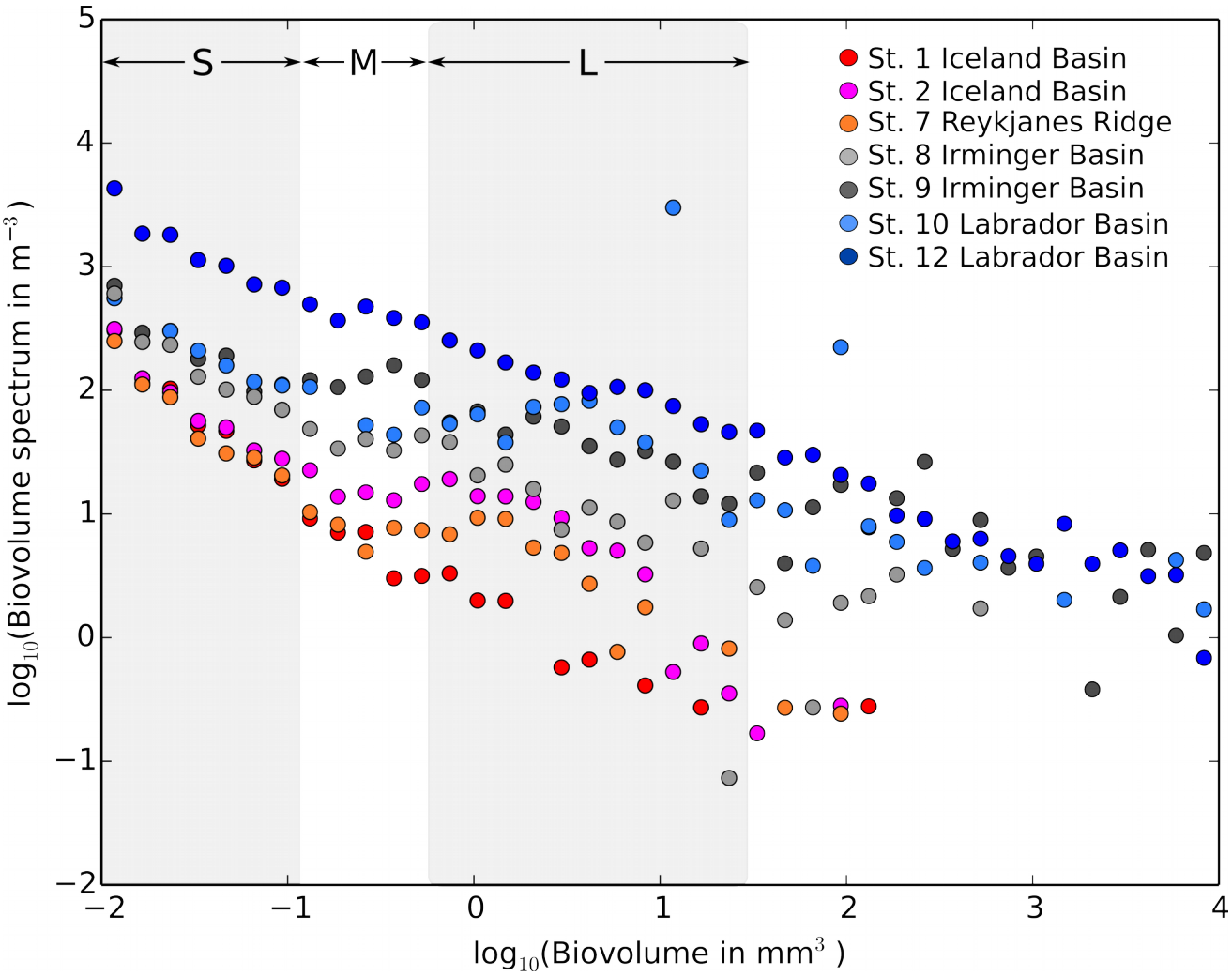

1000 Figure 3

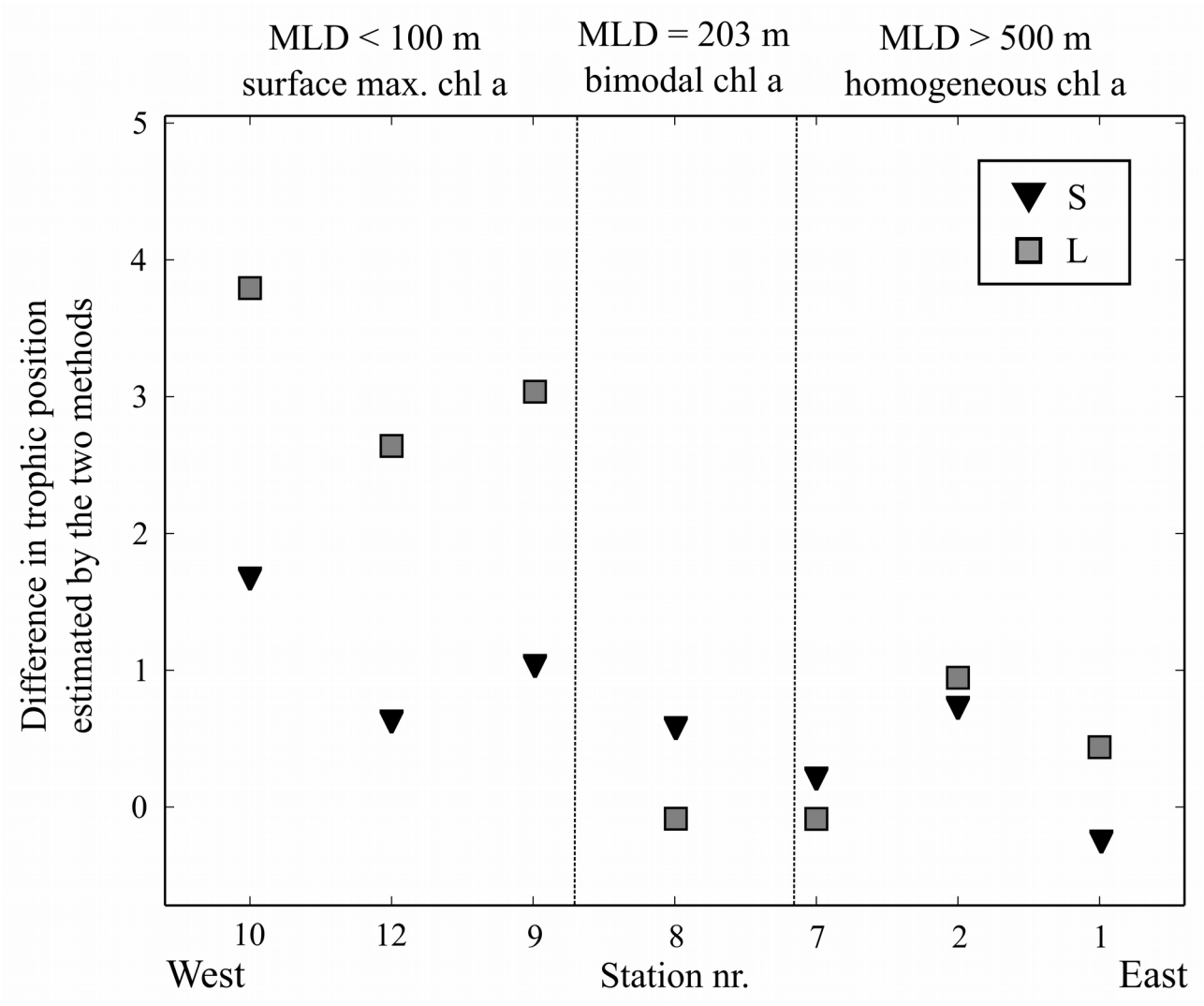

1002 Figure 4

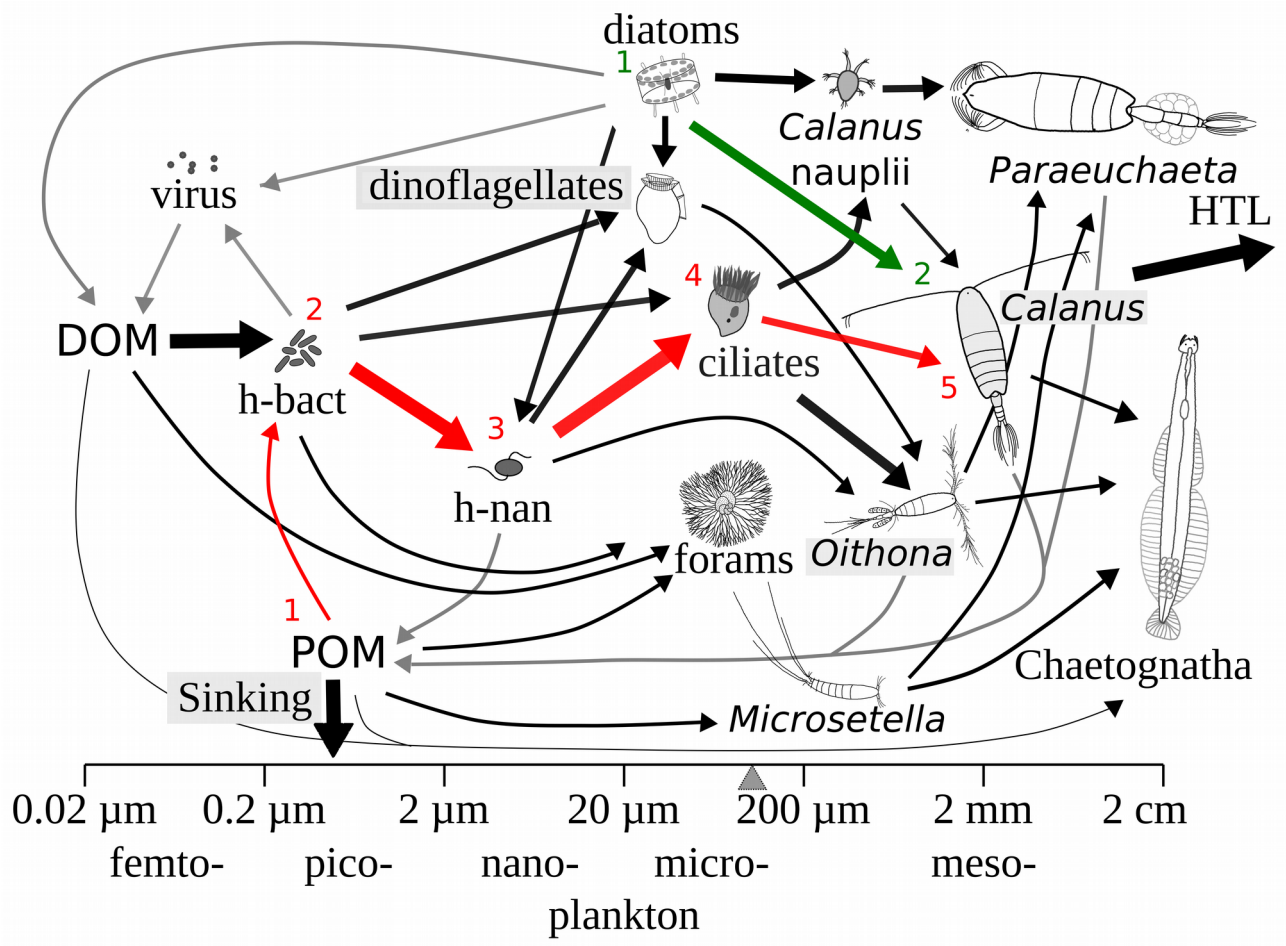

1003 Figure 5